

Crystal and molecular structure of dimethyl(L-tryptophyl-L-alaninato)tin(IV)-methanol (1/1) and Mössbauer spectroscopy studies of lattice dynamics of diorganotin(IV) dipeptide complexes †

Maria Assunta Girasolo,^a Lorenzo Pellerito,^a Gian Carlo Stocco^{*a} and Giovanni Valle^b

^a Dipartimento di Chimica Inorganica, Università di Palermo, via Archirafi 26, 90123 Palermo, Italy

^b Centro di Studio sui Biopolimeri, Dipartimento di Chimica Organica, Università di Padova, via Marzolo 1, 35131 Padova, Italy

The crystal and molecular structure of dimethyl(L-tryptophyl-L-alaninato)tin(IV)-methanol (1/1) has been determined by X-ray crystallography. The tin atom, bonding to two methyl carbons [Sn–C(1) 2.107(6), Sn–C(2) 2.121(8) Å; C(1)–Sn–C(2) 123.8(3)°], terminal amino nitrogen [Sn–N_{amino} 2.272(5) Å], deprotonated peptide nitrogen [Sn–N_{peptide} 2.064(5) Å] and terminal carboxylate [Sn–O_{carboxylate} 2.174(5) Å], has a five-coordinated trigonal-bipyramidal environment. An extended hydrogen-bond network gives rise to one-dimensional polymeric chains. The molecular dynamics of three tryptophan-containing dipeptide complexes with R₂Sn^{IV} (dipeptide dianion = Trp-AlaO, R = Me or Ph; dipeptide dianion = TrpTyrO, R = Me) have been investigated by variable-temperature ¹¹⁹Sn Mössbauer spectroscopy. The complexes behaved as Debye solids and, in particular, the calculated mean-square displacements of the tin atom confirm the occurrence of monomeric structures in such complexes interconnected through hydrogen bonds, which appear to be much stronger in SnMe₂(Trp-AlaO) and SnMe₂(Trp-TyrO) than in SnPh₂(Trp-AlaO).

Detailed X-ray crystallographic data for metal complexes can be used to assess the extent of association within the solids. In complexes of dipeptides and/or amino acids with metal ions, intermolecular association can be accomplished through bridging amino or carboxylate groups or through intermolecular hydrogen bonding. Variable-temperature ¹¹⁹Sn Mössbauer spectroscopy has been used to investigate lattice dynamics in monomeric and/or polymeric organotin complexes,¹ to probe the extent of intermolecular interactions in the solid and the structural motifs associated with it. Recently it has been also used to monitor the extent of stannylation of DNA and to survey the dynamic properties of lyophilized organotin–DNA condensates.²

The present study concerns the diorganotin(IV) (R = Me or Ph) moiety bonded to tryptophan-containing dipeptide dianions L-tryptophyl-L-alaninate (Trp-AlaO) and L-tryptophyl-L-tyrosinate (Trp-TyrO). The crystal structure of SnMe₂(Trp-AlaO)·MeOH has been determined, showing an extensive intermolecular association of monomers *via* hydrogen bonding. Variable-temperature Mössbauer spectroscopy has been used to assess the strength of such intermolecular interactions in the complexes.

Experimental

Syntheses

The compounds were synthesized by refluxing, for 4 h, freshly prepared SnMe₂O (1 mmol) and the dipeptide (1 mmol) in anhydrous methanol (50 cm³). After 30 min the solution was clear. The solvent was reduced to a small volume by rotary evaporation and the white solids dried *in vacuo* over P₄O₁₀ and analysed.³ The solids were recrystallized from anhydrous methanol. Colourless crystals were obtained from the solution of SnMe₂(Trp-AlaO) upon standing at ≈5 °C, while microcrystalline specimens were obtained for SnPh₂(Trp-AlaO) and SnMe₂(Trp-TyrO). Elemental microanalyses were per-

formed by Dipartimento di Chimica Organica ed Industriale, University of Milan (Found: C, 45.0; H, 5.6; N, 9.4. Calc. for C₁₇H₂₅N₃O₄Sn: C, 44.95; H, 5.55; N, 9.25. Found: C, 55.4; H, 4.95; N, 7.8. Calc. for C₂₆H₂₇N₃O₄Sn: C, 55.35; H, 4.8; N, 7.45. Found: C, 50.0; H, 5.2; N, 7.95. Calc. for C₂₃H₂₉N₃O₅Sn: C, 50.55; H, 5.35; N, 7.7%).

Authentication of the solvent content in the complexes (besides the structural determination for SnMe₂(Trp-AlaO)) was obtained by thermogravimetric measurements using a Mettler TA 3000 system in a pure nitrogen atmosphere in the temperature range 35–450 °C. A solution study of the complexes has been reported elsewhere.³

Physical techniques

Mössbauer spectra were recorded by using a model 639 multichannel analyser (TAKES, Bergamo, Italy) and the following components from MWE (Wissenschaftliche Elektronik GmbH, Munchen, Germany): MR250 driving unit, FG2 digital-function generator and MA250 velocity transducer, moved at a linear velocity and constant acceleration in a triangular waveform, and a Ba¹¹⁹SnO₃ source (10 MCi, Amersham, UK) at room temperature. The spectrometer was calibrated with a 95.2% ⁵⁷Fe-enriched iron foil (Dupont, MA) at room temperature, using a ⁵⁷Co–Pd source (10 MCi, Dupont, MA). The temperature-dependent spectra were obtained using a DN700 liquid-nitrogen cryostat with a DN1726 sample holder and model ITC 502 temperature controller (Oxford Instruments, UK). The temperature control was better than ±0.1 K.

Crystallography

Unit-cell dimensions for SnMe₂(Trp-AlaO) were determined and refined using the angular settings of 24 automatically centred reflections in the range 12 < 2θ < 24°. Intensity data were recorded using a 2θ scan from 4.5 to 56.0°. Intensities were measured with a Philips PW1100 diffractometer, T = 293 K, no absorption correction was applied and the structure was solved by direct methods using SHELXS 86⁴ and refined by full-matrix least-squares techniques with SHELX 76⁴ using

† Non-SI unit employed: Ci = 3.7 × 10¹⁰ Bq.

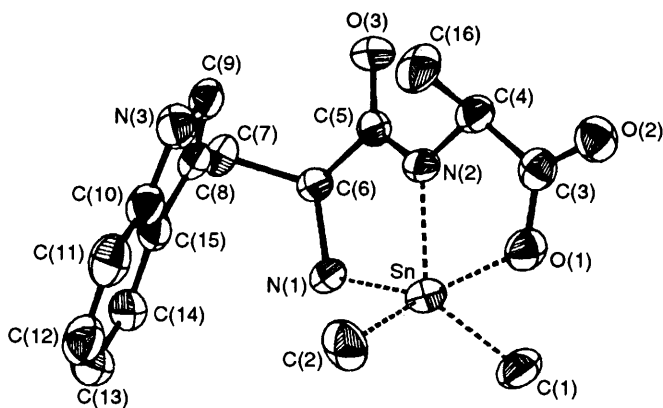


Fig. 1 Structure of $\text{SnMe}_2(\text{Trp-AlaO})$ and atomic numbering scheme

2205 reflections having $F > 3\sigma(F)$ and 214 refined parameters. The molecular graphics program used was ORTEP.⁵ Hydrogen atoms were partially located on a ΔF map but not refined. Data collection details and results of the refinements are summarized in Table 1, fractional coordinates in Table 2.

Complete atomic coordinates, thermal parameters and bond lengths and angles have been deposited at the Cambridge Crystallographic Data Centre. See Instructions for Authors, *J. Chem. Soc., Dalton Trans.*, 1996, Issue 1.

Results and Discussion

The crystal structures of organotin carboxylates including complexes with amino acids have been reviewed by Tiekink.⁶ Variable-temperature ^{119}Sn Mössbauer spectroscopy has been used to investigate the lattice dynamics in monomeric and/or polymeric organotin complexes.^{1,7}

Structure of $\text{SnMe}_2(\text{Trp-AlaO})$

Dimethyl(L-tryptophyl-L-alaninato)tin(IV)-methanol (1/1) is isostructural with dimethyltin dipeptide complexes previously reported.⁸ The dimethyltin(IV) moiety is bound by the terminal amino N atom, deprotonated peptide N atom and the terminal carboxylate group, with the chelating ligand forming two five-membered rings with the metal ion. The co-ordination about Sn is distorted trigonal bipyramidal with two methyl C atoms and $\text{N}_{\text{peptide}}$ in the equatorial plane, and N_{amino} and $\text{O}_{\text{carboxylate}}$ in the apical positions. The enclosed MeOH molecule has a site occupancy of 1 and takes part in an extended hydrogen-bond network of interactions in the crystal. Fig. 1 shows a view of the molecular structure along with the numbering scheme. Bond distances and angles are in Table 3, e.g. $\text{Sn}-\text{N}_{\text{amino}}$ 2.272(5), $\text{Sn}-\text{N}_{\text{peptide}}$ 2.064(5) Å, $\text{Sn}-\text{O}_{\text{carboxylate}}$ 2.174(5) Å, $\text{Sn}-\text{C}(1)$ 2.107(6) Å, $\text{Sn}-\text{C}(2)$ 2.121(8) Å and C-Sn-C (organometallic moiety) 123.8(3)°.

The axial angle $\text{O}(1)-\text{Sn}-\text{N}(1)$ [$151.5(2)^\circ$] deviates appreciably from linearity. The best mean co-ordination plane of the dipeptide is defined by atoms N(1), C(6), N(2), C(3), O(1), with minor deviations of +0.095 Å for C(5) and -0.0974 Å for C(4). The methyl group of the alanyl residue is in axial position [C(5)-N(2)-C(4)-C(16) 73.5(7), O(1)-C(3)-C(4)-C(16) 110.1(7)°].

The geometry, bond distances and angles of the portion of the tryptophyl residue not involved in the peptide bond are substantially in agreement with the values found for the amino acid either in the free or complexed form,⁹⁻¹¹ in Trp-containing derivatives¹² and complexes.¹³ The indole ring projects obliquely toward the chelate ring and forms an angle of 118.2° with the mean co-ordination plane N(1), C(6), N(2), C(3), O(1).

The conformation of the Trp residue can be described using the torsion angles in Table 4. Noticeably, $\chi^1 = \text{N}(1)-\text{C}(6)-\text{C}(7)-\text{C}(8)$ 64.0(7), $\chi^{2,1} = \text{C}(6)-\text{C}(7)-\text{C}(8)-\text{C}(9)$ 88.3(8),

Table 1 Crystallographic data and experimental details

Formula	$\text{C}_{17}\text{H}_{25}\text{N}_3\text{O}_4\text{Sn}$
<i>M</i>	454.11
Crystal symmetry	Orthorhombic
Space group	$P2_12_12_1$
<i>a</i> /Å	20.505(1)
<i>b</i> /Å	10.197(2)
<i>c</i> /Å	9.293(2)
<i>U</i> /Å ³	1943.1(6)
<i>Z</i>	4
<i>D_c</i> /Mg m ⁻³	15.4
Crystal dimensions/mm	0.3 × 0.3 × 0.5
$\lambda(\text{Mo-K}\alpha)$ /Å	0.710 73
μ/cm^{-1}	13.42
No. measured reflections	2672
No. independent reflections	2672
No. observed reflections [$F > 3\sigma(F)$]	2205
Ranges of <i>h, k, l</i>	0-27, 0-13, 0-12
<i>F</i> (000)	908
No. refined parameters	214
$ \Delta/\sigma _{\text{max}}$	0.52
$\Delta\rho_{\text{max}} \Delta\rho_{\text{min}}/e \text{ \AA}^{-3}$	0.95, -1.33
<i>R</i> '	0.021
<i>R</i>	0.038
<i>wR</i>	0.040
Goodness of fit	0.914
Weighting scheme, <i>w</i>	$1/[\sigma^2(F) + 0.0014 F^2]$

$R' = \Sigma[|F_o|^2 - |F_c|^2]/\Sigma|F_o|^2$; $R = \Sigma[|F_o| - |F_c|]/\Sigma|F_o|$; $wR = \Sigma[w(|F_o| - |F_c|)]/\Sigma(w|F_o|)$; goodness of fit = $[\Sigma w(F_o - F_c)^2/(N - P)]^{1/2}$, *N* = number of observed reflections, *P* = number of parameters.

Table 2 Positional parameters ($\times 10^4$) of the non-H atoms with estimated standard deviations in parentheses for $\text{SnMe}_2(\text{Trp-AlaO})$

Atom	<i>x</i>	<i>y</i>	<i>z</i>
Sn	1896(2)	433(4)	1523(5)
O(1)	2841(2)	289(5)	2578(5)
O(2)	3857(2)	1066(5)	2652(6)
O(3)	2570(2)	3379(4)	-1251(5)
N(1)	1242(3)	1193(5)	-265(6)
N(2)	2452(2)	1881(4)	568(6)
N(3)	1399(3)	5279(6)	2464(7)
C(1)	1978(4)	-1527(6)	832(9)
C(2)	1365(4)	1023(8)	3371(8)
C(3)	3285(3)	1098(6)	2196(7)
C(4)	3099(3)	2162(6)	1154(7)
C(5)	2252(3)	2549(6)	-600(7)
C(6)	1551(3)	2274(6)	-1085(7)
C(7)	1156(3)	3574(7)	-1010(8)
C(8)	1118(3)	4121(6)	478(8)
C(9)	1565(3)	4962(6)	1089(9)
C(11)	471(2)	4574(5)	4044(4)
C(12)	-103(2)	3843(5)	4088(4)
C(13)	-307(2)	3151(5)	2874(4)
C(14)	63(2)	3190(5)	1616(4)
C(15)	638(2)	3921(5)	1572(4)
C(10)	842(2)	4613(5)	2786(4)
C(16)	3103(4)	3509(6)	194(1)
O(4)	-204(4)	1874(7)	-1981(9)
C(17)	5(5)	1285(9)	-325(1)

C(5)-C(6)-C(7)-C(8) -61.6(7), O(3)-C(5)-C(6)-N(1) 176.2(5), $\chi^{2,2} = \text{C}(6)-\text{C}(7)-\text{C}(8)-\text{C}(15)$ -91.6(8)°. With respect to the $\text{C}^\alpha-\text{C}^\beta$ bond, $\text{C}^\beta-\text{C}^\gamma$ lies *gauche* relative to $\text{C}^\alpha-\text{CO}$ and $\text{C}^\alpha-\text{NH}_2$ thus corresponding to the *h* rotamer.¹⁴ Several examples of these rotamers have been observed in crystal structures¹⁵ where metal (mostly Cu^{2+})-aromatic ring interactions and ring-ring stacking interactions¹⁶ are a major factor for the stability of the folded structure.

The crystal structure of glycyl-L-tryptophanato-copper(II) dihydrate¹⁷ shows the side-chain aromatic ring occupying the space above the co-ordination plane, with a metal-aromatic ring distance of ca. 3.0-3.5 Å, which is less than the van der

Waals distance. Significantly, however, the square-planar copper(II) complex is sandwiched by two tryptophan residues, one from a neighbouring molecule.

The crystal packing of our complex (Fig. 2) does not show stacking of Trp side chains nor is the indole nitrogen involved in inter- or intra-molecular bonding to the organometallic moiety. In the absence of side chain-side chain interactions between the chelate ligands, there must be, as outlined in a general survey

of several factors influencing conformation by Vestues and Martin,¹⁴ a subtle stereochemical factor responsible for favouring an orientation of the side chain in the direction of the organometallic ion in this complex. Fig. 2 also affords a representation of the propagating hydrogen-bonded association the monomeric units which are related by the 2_1 screw-axis symmetry element. Hydrogen bonds play a significant role in determining the crystal packing of the complex and are reported in Table 5.

Each monomeric unit forms a weak hydrogen bond with a neighbouring molecule, through the N(1) atom of the coordinated amino group and the uncoordinated O(2) atom of the carboxylate group, in addition to a strong hydrogen bond linking N(3) of the indole ring to O(3) of the neighbouring peptide bond, the donor-hydrogen-acceptor angles being 170.6(3) and 155.1(4) $^\circ$ respectively, values in the range expected for such systems.²⁰ Moreover, the methanol molecules take part in a hydrogen bond with O(2) atoms of the carboxylate group. The first two link the monomers into infinite chains directed along 001 axis, the third along the 100 direction. The first two monomeric units are shifted by a cell length along the 010 axis, as the result they form a pattern of catenated molecules.

Exploitation of hydrogen bonds for the design and synthesis of specific structural motifs in the solid state has led to the formulation of the concepts underlying the field of crystal engineering.²¹⁻²³ Molecular recognition can be exerted by

Table 3 Bond distances (Å) and angles ($^\circ$)

(a) Co-ordination sphere

Sn-O(1)	2.174(5)	Sn-C(1)	2.107(6)
Sn-N(1)	2.272(5)	Sn-C(2)	2.121(8)
Sn-N(2)	2.064(5)		
C(1)-Sn-C(2)	123.8(3)	N(2)-Sn-C(2)	115.4(3)
N(2)-Sn-C(1)	120.3(3)	N(1)-Sn-C(2)	101.0(3)
N(1)-Sn-C(1)	98.5(2)	N(1)-Sn-N(2)	76.5(2)
O(1)-Sn-C(2)	96.4(2)	O(1)-Sn-C(1)	90.2(2)
O(1)-Sn-N(2)	75.6(2)	O(1)-Sn-N(1)	151.5(2)
Sn-O(1)-C(3)	117.7(4)	Sn-N(1)-C(6)	112.2(4)
Sn-N(2)-C(5)	122.8(4)	Sn-N(2)-C(4)	118.7(4)

(b) L-Tryptophyl-L-alaninate ligand

O(1)-C(3)	1.279(8)	C(6)-C(7)	1.555(9)
O(2)-C(3)	1.249(8)	C(7)-C(8)	1.49(1)
O(3)-C(5)	1.228(8)	C(8)-C(9)	1.378(9)
N(1)-C(6)	1.482(8)	C(8)-C(15)	1.429(8)
N(2)-C(4)	1.463(8)	C(11)-C(10)	1.395(6)
N(2)-C(5)	1.345(8)	C(11)-C(12)	1.395(7)
N(3)-C(9)	1.36(1)	C(12)-C(13)	1.395(6)
N(3)-C(10)	1.362(8)	C(13)-C(14)	1.395(6)
C(3)-C(4)	1.503(9)	C(14)-C(15)	1.395(7)
C(4)-C(16)	1.557(9)	C(15)-C(10)	1.395(6)
C(5)-C(6)	1.534(9)	O(4)-C(17)	1.39(1)
C(4)-N(2)-C(5)	118.5(5)	C(9)-N(3)-C(10)	107.3(6)
O(1)-C(3)-O(2)	123.9(6)	O(2)-C(3)-C(4)	118.4(6)
O(1)-C(3)-O(4)	117.6(6)	N(2)-C(4)-C(3)	109.2(5)
C(3)-C(4)-C(16)	109.4(6)	N(2)-C(4)-C(16)	110.7(5)
O(3)-C(5)-N(2)	125.9(6)	N(2)-C(5)-C(6)	115.4(5)
O(3)-C(5)-C(6)	118.6(5)	N(1)-C(6)-C(5)	112.6(5)
C(5)-C(6)-C(7)	108.6(5)	N(1)-C(6)-C(7)	112.9(5)
C(6)-C(7)-C(8)	112.7(5)	C(7)-C(8)-C(15)	129.9(6)
C(7)-C(8)-C(9)	125.3(6)	C(9)-C(8)-C(15)	104.8(5)
N(3)-C(9)-C(8)	111.5(6)	C(12)-C(11)-C(10)	120.0(4)
C(11)-C(12)-C(13)	120.0(4)	C(12)-C(13)-C(14)	120.0(4)
C(13)-C(14)-C(15)	120.0(4)	C(8)-C(15)-C(14)	132.7(4)
C(14)-C(15)-C(10)	120.0(4)	C(8)-C(15)-C(10)	107.2(5)
C(11)-C(10)-C(15)	120.0(4)	N(3)-C(10)-C(15)	109.0(4)
N(3)-C(10)-C(11)	130.9(5)		

Table 4 Torsion angles ($^\circ$)

Sn-N(2)-C(5)-C(6)	6.5(7)	C(6)-C(7)-C(8)-C(9)	88.3(8)
Sn-N(2)-C(4)-C(16)	-108.6(5)	C(6)-C(7)-C(8)-C(15)	-91.6(8)
Sn-N(2)-C(4)-C(3)	11.8(6)	C(7)-C(8)-C(9)-N(3)	-179.4(6)
C(4)-N(2)-C(5)-O(3)	1.0(9)	C(7)-C(8)-C(15)-C(10)	177.7(6)
C(4)-N(2)-C(5)-C(6)	-175.7(5)	C(7)-C(8)-C(15)-C(14)	-1.0(1)
C(5)-N(2)-C(4)-O(3)	-166.0(5)	C(15)-C(8)-C(9)-N(3)	0.5(8)
C(5)-N(2)-C(4)-C(16)	73.5(7)	C(9)-C(8)-C(15)-C(10)	-2.3(6)
C(9)-N(3)-C(10)-C(11)	179.2(6)	C(9)-C(8)-C(15)-C(14)	179.2(6)
C(9)-N(3)-C(10)-C(15)	-2.9(7)	C(12)-C(11)-C(10)-N(3)	177.5(5)
C(10)-N(3)-C(9)-C(8)	1.4(8)	C(12)-C(11)-C(10)-C(15)	0.0(7)
O(1)-C(3)-C(4)-N(2)	-11.0(8)	C(10)-C(11)-C(12)-C(13)	0.0(7)
O(2)-C(3)-C(4)-N(2)	169.9(5)	C(11)-C(12)-C(13)-C(14)	-0.0(7)
O(2)-C(3)-C(4)-C(16)	-68.7(8)	C(12)-C(13)-C(14)-C(15)	0.0(7)
O(1)-C(3)-C(4)-C(16)	110.1(7)	C(13)-C(14)-C(15)-C(8)	178.2(6)
O(3)-C(5)-C(6)-N(1)	176.2(5)	C(13)-C(14)-C(15)-C(10)	0.0(7)
N(2)-C(5)-C(6)-N(1)	-6.7(7)	C(8)-C(15)-C(10)-C(11)	-178.6(5)
N(2)-C(5)-C(6)-C(7)	119.1(6)	C(8)-C(15)-C(10)-N(3)	3.3(6)
O(3)-C(5)-C(6)-C(7)	-57.8(7)	C(14)-C(15)-C(10)-C(11)	-0.0(7)
C(5)-C(6)-C(7)-C(8)	-61.6(7)	C(14)-C(15)-C(10)-N(3)	-178.0(5)
N(1)-C(6)-C(7)-C(8)	64.0(7)		

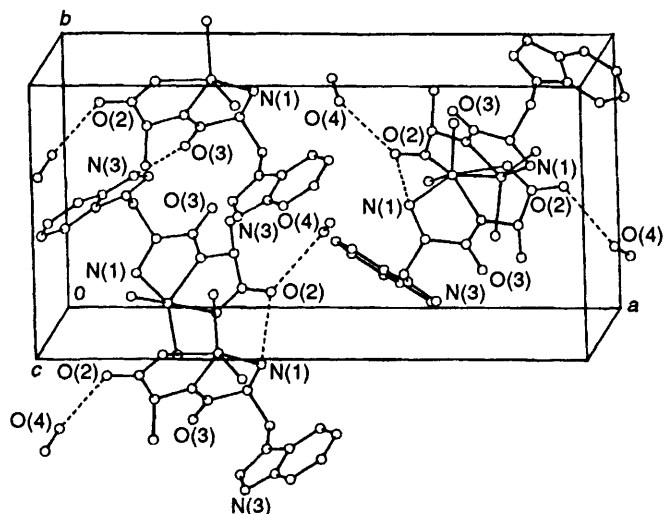


Fig. 2 The unit cell of $\text{SnMe}_2(\text{Trp-AlaO})\cdot\text{MeOH}$. Dashed lines indicate hydrogen bonds

Table 5 Intramolecular hydrogen-bond distances (Å) and angles (°). The second row of data for each bond gives values normalized following refs. 18 and 19

D-H...A	D-H	H...A	D...A	D-H...A
N(1)-H(1N1)...O(2 ^I)	1.016(5)	2.009(5)	3.016(7)	170.64(33)
	1.030	1.995		170.58
N(3)-H(1N3)...O(3 ^{II})	1.031(6)	1.817(4)	2.786(7)	155.14(38)
	1.030	1.818		155.16
O(1)-H(1O4)...O(2 ^{III})	1.022(7)	1.893(5)	2.915(9)	179(50)

Number of possible hydrogen bonds: 4. Symmetry codes: I $-x + \frac{1}{2}, -y, z - \frac{1}{2}$; II $-x + \frac{1}{2}, -y + 1, z + \frac{1}{2}$; III $x - \frac{1}{2}, -y + \frac{1}{2}, -z$.

hydrogen bonds in biological examples such as leucine zippers²⁴ in proteins and their synthetic analogues,²⁵ where co-ordinated copper(I) ions promote the assembly of double- and triple-stranded bipyridine oligomers.

Intermolecular hydrogen bonds between N(3) of the indole ring and O(3) of the carbonyl oxygen of the singly co-ordinated carboxylate group are found in the crystal structure of tricyclohexylstannyl indol-3-ylacetate, which crystallizes in the same space group $P2_12_12_1$ as that of our compound and the overall architecture of the crystal consists of one-dimensional arrays of helices.²⁶ The indole conformation closely resembles that found in $\text{SnMe}_2(\text{Trp-AlaO})$.

The conformation of both Trp and Tyr amino acids in $\text{SnMe}_2(\text{Trp-TyrO})$ has been previously investigated³ by ¹H NMR spectroscopy and rotamer population was calculated. In CD_3OD solution, for the C-terminal Tyr, the *h* rotamer accounted for 72% of the total population, while no such clear evaluation was possible for $\text{SnPh}_2(\text{Trp-AlaO})$.

Thermogravimetric analysis

Differential thermal gravimetry (DTG) measurements show a one-step solvent loss. For $\text{SnMe}_2(\text{Trp-AlaO})$ (see previous section) the weight loss in the range 199–207 °C amounts to 1 mol of MeOH per mol complex (Found: 5.55. Calc. 7.05%). Similarly, for $\text{SnMe}_2(\text{Trp-TyrO})$ a weight of loss of 6.80% (Calc. 5.85%) is indicative of 1 mol of MeOH per mol complex, while for $\text{SnPh}_2(\text{Trp-AlaO})$ a weight loss of 2.50% might suggest the retention of a water molecule (Calc. 3.20%).

¹¹⁹Sn Mössbauer spectroscopy

In the case of thin absorbers, behaving as Debye solids, the natural logarithm of the normalized total areas under the resonant peaks of the Mössbauer spectra, $\ln A$, investigated as function of the absolute temperature, may give useful information on the intermolecular interactions.^{7,27} Variable-temperature ¹¹⁹Sn Mössbauer spectroscopy was developed by several authors¹ as a structural probe in organotin chemistry. It is well established that, for thin absorbers and in the high-temperature limit $T \geq \theta_D/2$ (θ_D = Debye temperature of the investigated absorber), the function $\ln A(T)$ may be used to calculate, by appropriate computer software, several correlated parameters, which lead to conclusions on the extent of intermolecular interactions.²⁸ In particular, it is possible to obtain the recoil-free fraction (f_a) and the Debye temperature according to equation (1) where E_γ is the transition energy of

$$d(\ln A)/dT = d \ln f_a/dT = (-3E_\gamma^2/Mc^2k\theta_D^2) \quad (1)$$

the Mössbauer atom under investigation, M is the effective vibrating mass of the Debye solid, c is the velocity of light and k the Boltzmann constant.

The mean-square displacements as function of the absolute temperature, on the other hand, may be calculated from the function $f_a(T)$, which is correlated with the mean-square displacement, $\langle x^2 \rangle$, as in equation (2), where k = wavevector

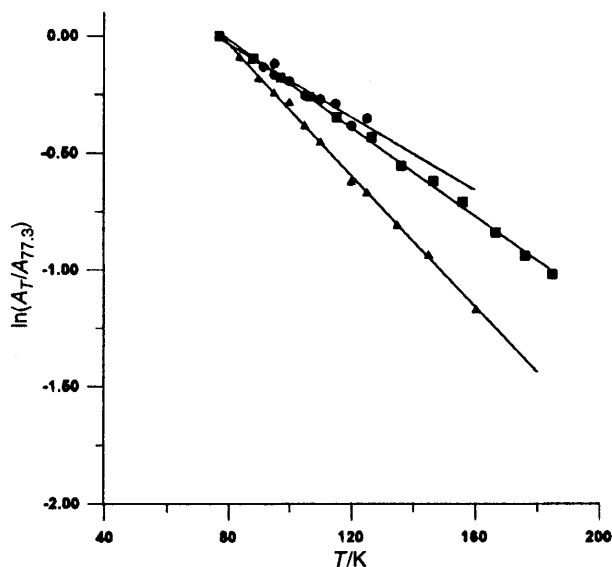


Fig. 3 Temperature dependence of the logarithm of the normalized areas under the resonant peaks for $\text{SnMe}_2(\text{Trp-AlaO})$ (■), $\text{SnMe}_2(\text{Trp-TyrO})$ (●) and $\text{SnPh}_2(\text{Trp-AlaO})$ (▲). Each full line represents the least-squares fit to the experimental data points. The corresponding equations are $\ln(A_T/A_{77.3}) = 0.748 - 0.00948T$, $0.596 - 0.0783T$ and $-1.430 - 0.014T$

$$d(\ln f_a)/dT = -k^2 \langle x^2 \rangle \quad (2)$$

of the γ ray, while the Debye cut-off frequency, ν_D , may be extracted by using equation (3).

$$\nu_D = k\theta_D/h \quad (3)$$

Finally, a preliminary determination of the recoil-free fraction of the source may lead to the absolute recoil-free fraction of the thin absorber.^{7,27}

Taking into account the $d(\ln A)/dT$ values, some further information about the structure of the solids can be extracted. In organotin(IV) dipeptide derivatives intermolecular association may occur through amino bridging groups,²⁸ bridging carboxylate groups,^{29,30} or through intermolecular hydrogen bonding. In some cases the contribution of hydrogen bonding can be more significant than the coordinative covalent bonding to the tin atom.³¹ Values of the slopes $d(\ln A)/dT$ higher than $-1.8 \times 10^{-2} \text{ K}^{-1}$ are representative of non-interacting monomeric tin-containing molecules, regardless of the coordination number of tin. Solids in which one-, two- and three-dimensional association or strongly hydrogen-bonded lattices may occur usually present $d(\ln A)/dT$ slopes lower than $-0.9 \times 10^{-2} \text{ K}^{-1}$. Weak intermolecular interactions will result in $d(\ln A)/dT$ slopes within the above-mentioned values.

The results obtained for the investigated complexes are reported in Table 6 and Figs. 3 and 4 show the representative functions $\ln A(T)$, $\ln f_a^{\text{rel,abs}}(T)$ and $\langle x^2 \rangle(T)$. The analysis of the data in Table 6 leads to several conclusions: (i) the θ_D values allow us to conclude that the investigated temperature ranges

Table 6 Tin-119 Mössbauer parameters and molecular dynamics of tin(tv) dipeptide derivatives

Compounds	Sample thickness/ $^{119}\text{Sn cm}^{-2}$	$\delta_{\text{av}}^a/\text{mm s}^{-1}$	$\Delta E_{\text{av}}^b/\text{mm s}^{-1}$	$\Gamma_{\text{av}}^c/\text{mm s}^{-1}$	No. data points	Temperature range/K	Corresponding area range ^d	$10^2 d(\ln A)/dT(\text{K}^{-1})$	θ_p^f/K	ν_D^g/cm^{-1}
$\text{SnMe}_2(\text{Trp-AlaO})$	0.443	1.11	2.73	0.84	12	77.3–185.0	0.173–0.061	–0.95 (0.998)	79.6 (79.5 ± 0.3)	55.3 (55.2 ± 0.2)
$\text{SnPh}_2(\text{Trp-AlaO})$	0.422	1.03	2.46	0.93	12	77.3–160.5	0.128–0.027	–1.41 (0.998)	52.6 (52.5 ± 0.2)	36.5 (36.4 ± 0.1)
$\text{SnMe}_2(\text{Trp-TyrO})$	0.492	1.12	2.78	1.03	9	77.3–125.3	0.048–0.038	–0.78 (0.993)	72.7 (72.5 ± 0.2)	50.5 (50.7 ± 0.2)

^a Isomer shift, $\delta \pm 0.03 \text{ mm s}^{-1}$, with respect to room-temperature CaSnO_3 averaged over the investigated temperature range. ^b Nuclear quadrupole splittings, $\Delta E \pm 0.02 \text{ mm s}^{-1}$, averaged over the investigated temperature range. ^c Averaged values, over the investigated temperature range, of the full widths at half height of the resonant peaks, respectively at lower and higher velocity with respect to the spectrum centroid. ^d The total area under the resonant peaks of the Lorentzians calculated according to $\text{area} = (\pi/2)\varepsilon\Gamma$, where ε = percentage of the resonant effect. ^e Slope of the normalized total area under the resonant peaks as a function of temperature; the correlation coefficients of the straight lines $\ln A$ versus T are given in parentheses. ^f Debye temperature obtained from $d(\ln A)/dT$ and from f_s^{abs} , in parentheses, together with the standard error. Effective vibrating masses have been assumed equal to the molecular weights for all the compounds. ^g Cut-off frequency calculated from $d(\ln A)/dT$ and from f_s^{abs} , in parentheses, together with the standard error.

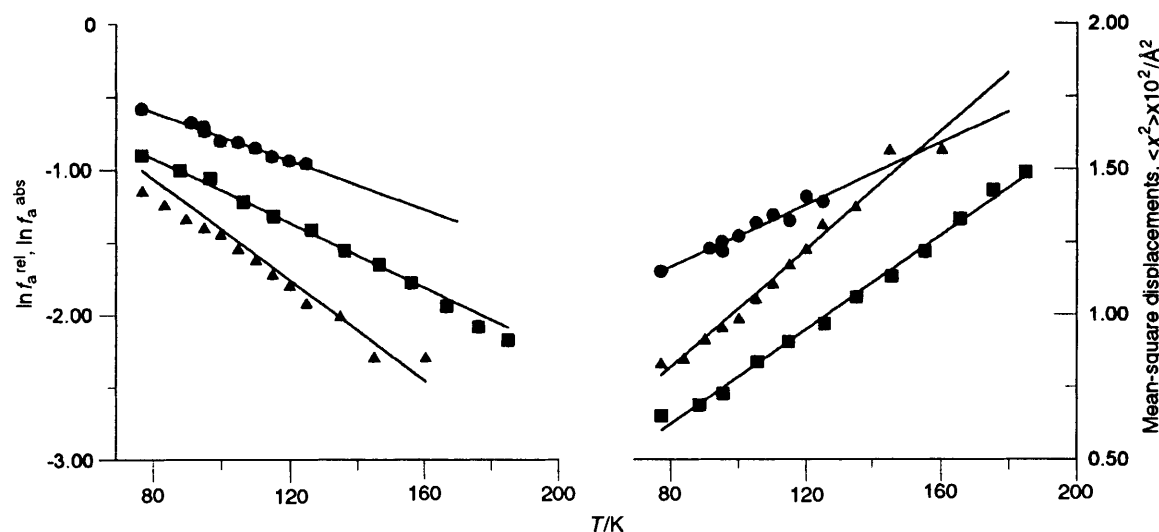


Fig. 4 Recoil-free fraction of the absorber ^{119}Sn nuclei, f_a , and mean-square displacements of the ^{119}Sn nuclei, $\langle x^2 \rangle$, as a function of temperature for $\text{SnMe}_2(\text{Trp-AlaO})$ (■), $\text{SnMe}_2(\text{Trp-TyrO})$ (●) and $\text{SnPh}_2(\text{Trp-AlaO})$ (▲). The lines are plots of $\ln f_a^{\text{rel}}(T)$ and related $\langle x^2 \rangle(T)$ as extracted from the slopes $d(\ln A_{100})/dT$; data points are absolute data, f_a^{abs} and corresponding $\langle x^2 \rangle$

Table 7 Slopes of functions $\ln A(T)$ for organotin(IV) compounds showing intermolecular hydrogen bonding

Compound	$10^2 d(\ln A_T/A_{77})/dT$	Ref.	Notes
$\{\text{SnPh}_3[\text{O}_2\text{CCH}(8\text{-C}_9\text{H}_6\text{NO})]\cdot\text{H}_2\text{O}\}_n$	-1.99	32	Monomeric, with hydrogen bonds generating helical chains
$\text{SnMe}_3(\text{O}_3\text{SPh})\cdot\text{H}_2\text{O}$	-1.71	33	Adjacent molecules weakly linked by hydrogen bonds to form one-dimensional infinite chains
$\text{SnMe}_2\text{Cl}[\text{SCH}_2(\text{NH}_2)\text{CO}_2\text{H}]\cdot\text{H}_2\text{O}$	-1.58	31	Dimeric hydrogen-bonded structure
$\text{SnMe}_2\text{Cl}[\text{SCMe}_2\text{CH}(\text{NH}_2)\text{CO}_2\text{H}]$	-1.46	31	Dimeric hydrogen-bonded structure
$\text{SnPh}_2(\text{Trp-AlaO})$	-1.41	This work	
$\text{SnMe}_2(\text{O}_2\text{CC}_5\text{H}_4\text{N})\cdot 2\text{H}_2\text{O}$	-1.27	34, 35	Adjacent molecules linked by three-dimensional network of hydrogen bonds
$\text{SnMe}_3[\text{OC}(\text{O})\text{CH}_2\text{NH}_2]$	-1.15	28	One-dimensional polymer with hydrogen bonds with interchain hydrogen bonds
$\text{SnMe}_2(\text{Trp-AlaO})$	-0.95	This work	
$\text{SnMe}_2(\text{ONHCOMe})_2$	-0.92	36	Adjacent molecules linked by hydrogen bonds
$\text{SnMe}_2(\text{Trp-TyrO})$	-0.78	This work	

may be considered in the high limit ($T \geq \theta_D/2$), which, together with the linearity of the $\ln A(T)$, $\ln f_a^{\text{rel,abs}}(T)$ and $\langle x^2 \rangle(T)$ functions confirms that the complexes behaved as Debye solids; (ii) the invariance both of δ and ΔE with temperature excludes any phase transition; (iii) the narrow linewidth Γ supports the occurrence of only one tin coordination site in all the derivatives; and (iv) the $d(\ln A)/dT$ and $\langle x^2 \rangle$ values are characteristic of monomeric hydrogen-bonded structures.

In Table 7 are reported slope data for some organotin(IV) derivatives, closely related to the complexes under investigation, for which hydrogen bonding has been well established through X-ray analysis and for which variable-temperature ^{119}Sn Mössbauer investigations have been carried out. In particular, the complex trimethyltin(IV) glycinate,²⁸ where both hydrogen bonding and a one-dimensional association *via* bridging amino groups are present, shows a $d(\ln A)/dT$ value of $-1.15 \times 10^{-2} \text{ K}^{-1}$. In contrast, in triphenyltin(IV) quinolin-8-yloxyacetate hydrate,³² where there is no evidence for intermolecular carboxylate bridging giving rise to intermolecular association, while an extensive hydrogen-bond network is promoted by tin(IV)-co-ordinated water molecules, generating a helical chain, $d(\ln A)/dT = -1.99 \times 10^{-2} \text{ K}^{-1}$. Comparison of the $d(\ln A)/dT$ values of the diorganotin(IV) dipeptide complexes in this work with those previously reported, allows us to conclude that $\text{SnMe}_2(\text{Trp-TyrO})[d(\ln A)/dT = -0.78 \times 10^{-2} \text{ K}^{-1}]$ and the crystallographically characterized $\text{SnMe}_2(\text{Trp-AlaO})[d(\ln A)/dT = -0.95 \times 10^{-2} \text{ K}^{-1}]$ are both monomeric units with strong intermolecular hydrogen bonding, while in the case of

$\text{SnPh}_2(\text{Trp-AlaO})[d(\ln A)/dT = -1.41 \times 10^{-2} \text{ K}^{-1}]$ the monomeric units are more weakly hydrogen bonded.

Acknowledgements

Financial support by Ministero dell' Università e della Ricerca Scientifica e Tecnologica, Rome, is gratefully acknowledged.

References

- 1 K. C. Molloy and K. Quill, *J. Chem. Soc., Dalton Trans.*, 1985, 1417; K. C. Molloy, S. J. Blunden and R. Hill, *J. Chem. Soc., Dalton Trans.*, 1988, 1259 and refs. therein; P. G. Harrison, K. Lambert, T. J. King and B. Magee, *J. Chem. Soc., Dalton Trans.*, 1983, 363; O. A. Bamgboye, T. T. Bamgboye and P. G. Harrison, *J. Organomet. Chem.*, 1986, **306**, 17 and refs. therein; B. King, H. Eckert, D. Z. Denney and R. H. Herber, *Inorg. Chim. Acta*, 1986, **122**, 45; R. H. Herber, *Phys. Rev. B*, 1983, **27**, 4013; R. H. Herber, A. Shanzer and J. Libman, *Organometallics*, 1984, **3**, 586 and refs. therein.
- 2 R. Barbieri, G. Ruisi, A. Silvestri, A. M. Giuliani, A. Barbieri, G. Spina, F. Pieralli and F. Del Giallo, *J. Chem. Soc., Dalton Trans.*, 1995, 467 and refs. therein.
- 3 M. A. Girasolo, G. Guli, L. Pellerito and G. C. Stocco, *Appl. Organomet. Chem.*, 1995, **9**, 241.
- 4 G. M. Sheldrick, (a) SHELXS 86, Program for Solution of Crystal Structures, University of Göttingen, 1986; (b) SHELX 76, Program for Crystal Structure Determination, University of Cambridge, 1976.
- 5 C. K. Johnson, ORTEP, Report ORNL-3794, Oak Ridge National Laboratory, Oak Ridge, TN, 1965.
- 6 E. R. T. Tiekink, *Appl. Organomet. Chem.*, 1991, **5**, 1.

- 7 R. V. Parish, *Mössbauer Spectroscopy Applied to Inorganic Chemistry*, ed. G. J. Long, Plenum, New York, 1984, vol. 1, p. 549.
- 8 G. C. Stocco, G. Guli and G. Valle, *Acta Crystallogr., Sect. C*, 1992, **48**, 2116.
- 9 T. Takigawa, T. Ashda, Y. Sasada and M. Kakudo, *Bull. Chem. Soc. Jpn.*, 1966, **39**, 2369.
- 10 K. Aoki and H. Yamazaki, *J. Chem. Soc., Dalton Trans.*, 1987, 2017.
- 11 K. Henrick, R. W. Matthews and P. A. Tasker, *Acta Crystallogr., Sect. B*, 1978, **34**, 935.
- 12 R. P. Ash, J. R. Herriott and D. A. Deranleau, *J. Am. Chem. Soc.*, 1977, **99**, 4471.
- 13 L. P. Battaglia, A. Bonamartini Corradi, G. Marcotrignano, L. Menabue and G. C. Pellacani, *J. Am. Chem. Soc.*, 1980, **102**, 2663.
- 14 P. I. Vestues and R. B. Martin, *J. Am. Chem. Soc.*, 1980, **102**, 7906.
- 15 M. Cotrait and Y. Barrans, *Acta Crystallogr., Sect. B*, 1974, **30**, 510.
- 16 T. Sugimori, K. Shibakawa, H. Masuda, A. Odani and O. Yamauchi, *Inorg. Chem.*, 1993, **32**, 4951.
- 17 M. B. Hursthouse, S. A. A. Jayaweera, H. Milburn and A. Quick, *J. Chem. Soc., Dalton Trans.*, 1975, 2569.
- 18 G. A. Jeffrey and L. Lewis, *Carbohydr Res.*, 1978, **60**, 179.
- 19 R. Taylor and O. Kennard, *Acta Crystallogr., Sect. B*, 1983, **39**, 133.
- 20 R. Taylor, O. Kennard and V. Werner, *J. Am. Chem. Soc.*, 1983, **105**, 5761; 1984, **106**, 244.
- 21 S. Subramanian and M. J. Zawarotko, *Coord. Chem. Rev.*, 1994, **137**, 357.
- 22 C. B. Aakeröy and M. Nieuwenhuyzen, *J. Am. Chem. Soc.*, 1994, **116**, 10983.
- 23 C. B. Aakeröy and K. R. Seddon, *Chem. Soc. Rev.*, 1993, 397.
- 24 K. T. O'Neil, R. H. Hoess and W. F. Degrado, *Science*, 1990, **249**, 774.
- 25 R. Kramer, J.-M. Lehn and A. Marquis-Rigault, *Proc. Natl. Acad. Sci. USA*, 1993, **90**, 5394.
- 26 K. C. Molloy, T. G. Purcell, E. Hahn, H. Schumann and J. J. Zuckerman, *Organometallics*, 1986, **5**, 85.
- 27 R. Barbieri, A. Silvestri, A. Barbieri, G. Ruisi, F. Huber and C. D. Hager, *Gazz. Chim. Ital.*, 1994, **124**, 187.
- 28 B. Y. K. Ho, K. C. Molloy, J. J. Zuckerman, F. Reidinger and J. A. Zubieta, *J. Organomet. Chem.*, 1980, **187**, 213.
- 29 B. Y. K. Ho and J. J. Zuckerman, *J. Organomet. Chem.*, 1973, **49**, 1.
- 30 J. A. Zubieta and J. J. Zuckerman, *Prog. Inorg. Chem.*, 1978, **14**, 251.
- 31 K. C. Molloy, J. J. Zuckerman, G. Domazetis and B. D. James, *Inorg. Chim. Acta*, 1981, **54**, L217.
- 32 V. G. Kumar Das, C. Wei and S. Weng Ng, *J. Organomet. Chem.*, 1987, **322**, 33.
- 33 P. G. Harrison, R. C. Phillips and J. A. Richards, *J. Organomet. Chem.*, 1976, **114**, 47.
- 34 P. G. Harrison and R. C. Phillips, *J. Organomet. Chem.*, 1979, **182**, 37.
- 35 P. G. Harrison, R. C. Phillips and E. W. Thornton, *J. Chem. Soc., Chem. Commun.*, 1977, 604 and refs. therein.
- 36 P. G. Harrison, T. J. King and R. C. Phillips, *J. Chem. Soc., Dalton Trans.*, 1976, 2317.

Received 13th October 1995; Paper 5/06795B